Heliyon 10 (2024) e27993

Contents lists available at ScienceDirect

Heliyon

journal homepage: www.cell.com/heliyon

Research article

Performance of ATT and UDFF in the diagnosis of non-alcoholic fatty liver: An animal experiment☆

Huihui Chen [a,1], Huiming Shen [a,1], Jiahao Han [a], Pingping Wang [a], Danlei Song [a], Hongyuan Shen [a], Xiaoying Wei [b], Bingjie Yang [a,**], Jia Li [a,*]

[a] Department of Ultrasound, Zhongda Hospital, Medical School, Southeast University, Nanjing, 210009, China
[b] Department of Pathology, Zhongda Hospital, Medical School, Southeast University, Nanjing, 210009, China

ARTICLE INFO

Keywords:
Non-alcoholic fatty liver disease
Ultrasound
Animal model
Bama minipigs
Pathological biopsy

ABSTRACT

Objective: To establish a Bama minipigs model with Non-Alcoholic Fatty Liver (NAFL) induced by a high-fat diet and investigate the application of attenuation coefficient (ATT) and ultrasound-derived fat fraction (UDFF) in the diagnosis of NAFL.
Methods: Six-month-old male Bama minipigs were randomly divided into normal control and high-fat groups (n = 3 pigs per group), and fed with a control diet and high-fat diet for 32 weeks. Weight and body length were measured every four weeks, followed by quantitative ultrasound imaging (ATT and UDFF), blood biochemical markers, and liver biopsies on the same day. Using the Non-Alcoholic Fatty Liver Disease (NAFLD) Activity Score (NAS) as a reference, we analyzed the correlation between ATT, UDFF, and their score results.
Results: Compared with the normal control group, the body weight, body mass index (BMI), and serum levels of triglyceride (TG), total cholesterol (TC), high-density lipoprotein cholesterol (HDL-C), and low-density lipoprotein cholesterol (LDL-C) in the High-fat group were significantly different at Week 12 ($P < 0.05$). Spearman correlation analysis showed that the ATT value was significantly correlated with NAS score ($r = 0.76$, $P < 0.001$), and the UDFF value was significantly correlated with NAS score ($r = 0.80$, $P < 0.001$). The optimal cut-off value of ATT and UDFF were 0.59 dB/cm/MHz and 5.5%, respectively. These values are optimal for diagnosis of NAFL in Bama minipig model.
Conclusion: ATT and UDFF have a high correlation with steatosis, and can be used as a non-invasive method for early screening of hepatic steatosis, which can dynamically monitor the change of disease course.

1. Introduction

Research has shown that the Asia-Pacific region accounts for more than 60% of the world's deaths due to liver disease, and NAFLD caused more than 12% of the deaths due to cirrhosis in the region [1]. NAFLD, including NAFL and nonalcoholic steatohepatitis

☆ Supported by Nanjing Health Commission, China (project number: YKK21275).
* Corresponding author. Department of Ultrasound, Zhongda Hospital, Medical School, Southeast University, Nanjing, China.
** Corresponding author. Department of Ultrasound, Zhongda Hospital, Medical School, Southeast University, Nanjing, China.
E-mail addresses: 15150690039@163.com (B. Yang), 13951609892@163.com (J. Li).
[1] Co-first Author.

https://doi.org/10.1016/j.heliyon.2024.e27993
Received 15 December 2023; Received in revised form 1 March 2024; Accepted 10 March 2024
Available online 18 March 2024

(NASH) [2], is one of the main causes of liver dysfunction [3]. NASH is a more severe form of NAFLD, which can lead to liver fibrosis and cirrhosis [4]. However, fibrosis progression has been found not only in NASH, but in NAFL [2,5]. Since NAFL is quite common and is expected to increase further over the next decade [6], but aside from lifestyle changes, diet changes, and possible bariatric surgery, there is no effective medical intervention that can completely reverse the disease [7]. A major obstacle to the development of NAFL therapy is the lack of preclinical disease models [8]. Therefore, we need to establish preclinical models to understand the pathophysiology and therapeutic mechanisms of NAFL. Animal NAFL models should develop a liver phenotype similar to human disease, mainly characterized by microcystic steatosis and hepatocyte swelling. At present, research on establishing fatty liver models mainly involves using mouse or guinea pig models [9–11]. In contrast, the anatomy and physiology of the liver and digestive system of pigs are more similar to those of humans [12]. In a recent study, a pig model of pediatric NAFLD was established to investigate the impact of dietary fat composition on bile acid metabolism and the extent of liver injury [13]. Thus, the Bama minipigs were selected as the experimental animal in this study.

Though NAFL can be diagnosed by imaging examination, the results still depend on the liver biopsy which is the gold standard. However, the invasive nature of the biopsy method could cause complications such as bleeding and infection, and which may delay result due to pathology reports [14]. Therefore, non-invasive and rapid imaging methods are needed to solve this problem. In recent years, quantitative ultrasound (QUS) technology has developed rapidly. ATT (Hitachi) adopts dual-frequency amplitude difference algorithm, its advantage lies in its ability to better eliminate the influence of structures along the propagation path, such as the microvascular system on changes of sound intensity. UDFF(Siemens) is an algorithm based on attenuation and back scattering, which refers to the module of the integrated body to correct the system effect. At present, there are few studies on ATT and UDFF in quantitative fatty liver. Therefore, we will evaluate the efficiency of the emerging.

ATT and UDFF in the early diagnosis of NAFL. Firstly, to establish the NAFL model of Bama minipigs induced by high-fat diet, which provided an experimental basis for the application of Bama minipigs in NAFL disease. Then, histopathological biopsy was used as the gold standard to evaluate the correlation between ATT, UDFF, and pathological results. This exploration aimed to determine the potential application value of QUS technology in hepatic steatosis and establish a foundation for further clinical research.

2. Materials and methods

2.1. Animal and feed preparation

6-month-old ordinary grade Bama minipigs were purchased from Wu Xi Hengtai (Wu Xi, China, SCCK(SU)2021–0021), with an initial weight between 24 and 27 kg. They were randomly divided into a high-fat group (HF, n = 3) and a normal control group (NC, n = 3) and given one week of environmental adaptation time. In order to maintain consistency, the pigs used in the experiment were all male. All animal procedures were approved by the Laboratory Animal Committee of the University, China (Ethics approval No20210625006). And this study followed recommendations by the National Research Council and the American Veterinary Medical Association's panel on euthanasia.

The NC group was fed an ordinary diet, while the HF group was fed a high-fat diet (the proportion of nutrients in experimental feed is shown in Table 1). The body weight and length of the experimental miniature pigs were measured every four weeks. The frequency of feeding was two times/day; the diet was 4% of the average pig weight of the month, and free drinking water. The 12-h light/dark cycle was maintained at a temperature of 19–22 °C and a relative humidity of 65%–75% throughout the study period. In order to minimize the pain of the animals, during the whole experiment, animals were treated humanely and with due consideration for their suffering (such as selecting of trained animal researchers and anesthesiologists, etc.). The Experimental Animal Committee of Southeast University approved the animal experiment procedure.

2.2. Ultrasonic equipment and data quality

The ultrasonic imaging equipment is the ARIETTA 850 ultrasonic diagnostic instrument (Fujifilm Healthcare; Tokyo, Japan) and ACUSON Sequoia ultrasonic diagnostic instrument (ACUSON Sequoia US system; Siemens, Germany).

In order to facilitate the transfer of the experimental pigs to the examination bed and cooperate with the examination, the minipigs were anesthetized intraperitoneal with 3% sodium pentobarbital. Food intake was stopped 4–8 h before anesthesia. The dosage of anesthetic (30 mg/kg) was determined according to the weight of the month, and abdominal ultrasound scanning would be started

Table 1
Dietary components of the two groups.

Contents	NC group (n = 3)	HF group (n = 3)
Crude Protein (%)	15.1	22.9
Crude fat (%)	4	34.1
Crude fiber (%)	3.9	3
Crude ash (%)	4.1	4.4
Calcium (%)	0.7	1.1
total phosphorus (%)	0.5	0.7

Abbreviations: NC, normal control; HF, high fat.

after entering the anesthesia state. The upper and lower limbs of the minipigs were fixed upward and downward, respectively, fully exposing the lower rib margin. Before scanning, the hair on the epidermis of the scanned part should be removed and cleaned. This preparation is necessary to avoid any interference with the subsequent probe scanning.

ATT measurement : Selected the abdominal convex array ultrasonic probe and set the frequency to 2.5–3.5 MHz. The proper intercostal space scan was performed to adjust the appropriate depth and gained in two dimensions images to achieve the best clarity (Fig. 1A), and then saved type B-model liver and kidney images with the same parameters (Fig. 1B). When measuring ATT, kept the sampling frame at least 1.5–2.0 cm below the liver capsule [15] and tried to make it perpendicular to the horizontal line. Selecting regions of interest (ROI) should avoid gallbladder, bile duct, large blood vessels, and rib sound shadow. At least five valid ATT values were measured to obtain the median value and quartile. For the accuracy of ATT measurement values, Hitachi suppliers provide confidence factor VsN, which is recommened to be above 50%. In addition, according to the guidelines, the ratio of quartile to median (IQR/M) should be less than 30%. ATT can accurately measure the ATT within the ROI, the yellow solid line (Fig. 1C).

UDFF measurement : DAX probe was used to scan the proper intercostal space, the horizontal cursor was placed on the liver capsule, and the solid yellow line was basically vertical. ROI sampling frame avoided sound shadows of large blood vessels, bile ducts, gallbladder, and ribs (Fig. 1D). A total of six UDFF values were measured, and the UDFF value was valid if IQR/M < 0.3. UDFF assesses hepatic steatosis by processing acoustic radiofrequency signals returned from liver tissue to estimate attenuation and backscattering coefficients, since fat vesicles in liver cells have different characteristic impediments compared to normal liver tissue.

2.3. Calculation of hepatorenal index

The software for calculating hepatorenal index (HRI) is ImageJ (V1.8.0.112, National Institutes of Health, America, https://imagej.nih.gov/ij/). It is readily available, and it has been used in previous studies to verify HRI [16,17]. The ImageJ selection tool displays rectangles, circles, or ellipses. This tool is used to select ROI. The program quickly performs histogram analysis of the selected ROI and displays average brightness and pixel size by the Measure feature. Renal ROI was limited to the renal cortex as much as possible. The liver ROI (basically at the same depth as the renal ROI) approximated the size of the kidney ROI and tried to avoid visible bile ducts, blood vessels, and artifact areas.

2.4. Blood biochemical detection

This study measured serum indexes of liver and lipid metabolism. The changes in blood indexes of miniature pigs were monitored. A linear array ultrasonic probe was selected to distinguish arteriovenous according to Doppler angiography. The anterior vena cava (located in the lower neck area) was identified by ultrasound images, and blood was drawn after wiping the corresponding epidermis with iodophor, 3–5 ml of blood was collected in a disposable EDTA vacuum tube (Becton Dickinson, USA). Plasma samples were centrifuged at 4000 rpm at 4 °C for 10 min using a centrifuge (Anke, China). Then, biochemical immunoassay equipment Cobas8000DM (Roche Diagnostics, Switzerland) was used to detect albumin (ALB), globulin (GLB), alanine aminotransferase (ALT), aspartate aminotransferase (AST), gamma-glutamate transpeptidase (GGT), triglyceride (TG), total cholesterol (TC), high-density lipoprotein cholesterol (HDL-C), and low-density lipoprotein cholesterol (LDL-C).

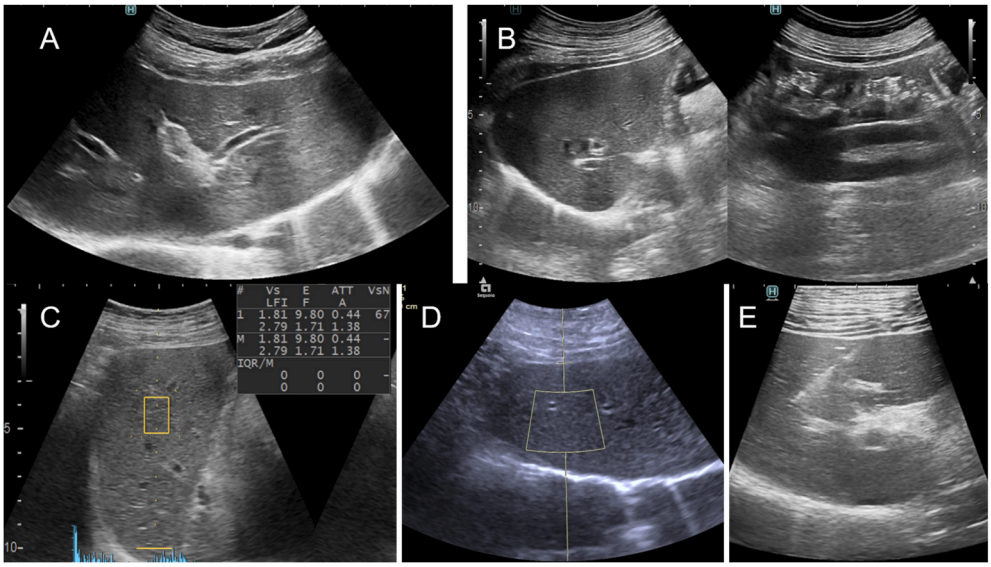

Fig. 1. Representative ultrasound images. (A) Two-dimensional image of the liver from Hitachi ultrasound equipment. (B) Two-dimensional image of the liver and kidney under the same parameter from Hitachi ultrasound equipment. (C) Representative image of Hitachi ultrasound equipment ATT measurement. (D) Representative image of Siemens ultrasound equipment UDFF measurement. (E) Screenshot of ultrasound-guided puncture.

2.5. Histopathological assessment

Hepatocyte steatosis is the accumulation of fat droplets in the form of triglycerides in the liver cells. When the accumulation of fat droplets occurs in >5% of hepatocytes, the histological diagnosis is NAFL. It can be graded according to the percentage of steatogenic hepatocytes: mild, 0–33%; moderate, 33–66%; severe, >66%. In severe cases, steatosis can occupy the entire acinar [18].

The pathological biopsy was performed by ultrasound-guided percutaneous biopsy of the liver (Fig. 1E). During the puncture, the pig was kept in the supine position with the forelimbs elevated. The ultrasound probe was placed in the right intercostal space for scanning, and the images showed the outline, section, arteries, and veins of the liver. The puncture path should be chosen to avoid the gallbladder and macroscopic hepatic vessels. By comparing the previous attenuation images and trying to find the same part of the liver region, the puncture point was selected and marked. An experienced doctor held the "ACHIEVE Tissue biopsy needle" (Merit Medical System Inc., USA) at the selected puncture site and obliquely entered the skin, subcutaneous fat layer, muscle layer, and liver capsule. After reaching a certain depth (the depth is the same as that of ultrasound attenuation imaging), the needle core was quickly pressed into the liver parenchyma, at which time the trocar automatically cut the liver tissue. The obtained liver tissues were fixed in 10% formalin solution and stained by Hematoxylin-eosin (HE). All specimens were analyzed by two independent pathologists who did not know the clinical and experimental characteristics of the tested subjects. NAS scores were used: the sum of scores for hepatic steatosis (0–3), lobular inflammation (0–3), and hepatocellular balloon (0–2) [19]. Since a NAS score of 4 or greater suggests the possibility of NASH [20], a NAS score of 1 or higher but less than 4 was considered indicative of NAFL. The average values of the scores analyzed by 2 independent pathologists will be calculated. The HE-stained slides were observed by an inverted microscope with a 40× objective lens (Olympus IX71, Japan).

2.6. Statistical analysis

Statistical analysis was performed by SPSS (Statistical Package for Social Science) version 24 (IBM, Armonk, NY) and GraphPad Prism 9 (GraphPad Software). Body weight, BMI, and blood biochemical test data were expressed as mean ± SD, while ATT and UDFF values were expressed as median and quartile. Independent sample T-test was used to analyze the body weight, BMI, and laboratory data of each group of miniature pigs. Spearman correlation method was used to evaluate the relationship between ATT, UDFF values, and liver histological scores. The diagnostic performance of ATT and UDFF (area under the curve (AUC), sensitivity, specificity) was evaluated by receiver operating characteristic (ROC) analysis with pathological scores as the reference standard. $P < 0.05$ was considered statistically significant.

3. Results

3.1. Phenotypic changes

3.1.1. Changes in body weight and BMI

The phenotypic characteristics of the two groups of minipigs are shown in Table 2. Compared with the NC group, the body weight and BMI of pigs after high-fat diet induction were significantly increased ($P < 0.05$, $P < 0.01$). Statistically significant differences in body weight (Fig. 2A) and BMI (Fig. 2B) of minipigs began to appear between the two groups at the 12th week of the experiment.

Table 2
Phenotypic characteristics of Bama minipigs in two groups ($\bar{X} \pm S$).

characteristic	NC group (n = 3)	HF group (n = 3)	P value
Basic physical			
Original weight(kg)	24.13 ± 1.19	25.67 ± 1.40	0.222
Final weight(kg)	58.80 ± 2.09	70.60 ± 1.12	< 0.05
Original BMI(kg/m^2)	29.80 ± 1.47	30.98 ± 1.06	0.323
Final BMI(kg/m^2)	54.36 ± 1.14	63.4 ± 0.42	< 0.05
laboratory examination (Week 16)			
TG(mmol/L)	0.30 ± 0.01	1.63 ± 0.07	< 0.001
TC(mmol/L)	3.22 ± 0.63	9.61 ± 1.54	< 0.01
HDL-C(mmol/L)	1.30 ± 0.38	2.88 ± 0.14	< 0.01
LDL-C(mmol/L)	1.77 ± 0.35	5.67 ± 1.15	< 0.05
ALT(U/L)	50.50 ± 5.31	43.00 ± 2.00	0.123
AST(U/L)	19.67 ± 1.70	24.67 ± 7.58	0.415
GGT(U/L)	71.67 ± 11.10	59.33 ± 8.26	0.276
ALB(g/L)	45.10 ± 1.18	43.73 ± 1.55	0.291
GLB(g/L)	23.80 ± 2.70	24.53 ± 1.88	0.719

Abbreviations: NC, normal control; HF, high fat; TG, Triglyceride; TC, total cholesterol; HDL-C, high-density lipoprotein cholesterol; LDL-C, low-density lipoprotein cholesterol; ALT, alanine aminotransferase; AST, aspartate aminotransferase; GGT, gamma-glutamate transpeptidase; ALB, albumin; GLB, globulin.

3.1.2. Changes in index of hematology

Laboratory results (Week 16) are shown in Table 2. Compared with the NC group, the serum levels of TG, TC, HDL-C, and LDL-C in the HF group showed statistical differences in a certain period. Among them, TG levels (Fig. 3A) showed statistically significant differences in the 4th week of high lipid induction ($P < 0.001$) and also in the subsequent 12th and 16th weeks ($P < 0.01$, $P < 0.001$). TC levels (Fig. 3B) were statistically different from 4 to 20 weeks after high-fat diet induction ($P < 0.05$, $P < 0.01$). HDL-C levels (Fig. 3C) were statistically different from 4 to 24 weeks after high-fat diet induction ($P < 0.05$, $P < 0.01$). LDL-C levels (Fig. 3D) were statistically different from 8 to 20 weeks ($P < 0.05$). The above serum markers in the high-fat group were significantly higher than those in the NC group at Week 12 and 16. However, for indicators related to liver function, the transaminases ALT, AST, and GGT were not statistically significant between the HF group and the NC group. There was also no statistical difference between ALB and GLB in the two groups.

3.2. Histopathological observation of liver

After 32 weeks of the experiment, HE staining results under light microscope showed that the liver lobules in the NC group were clearly outlined, the liver cell cords were neatly arranged, the boundaries were clear, the nuclear circle was located in the center of the cells, and the cytoplasm was abundant. Red blood cells might be due to congestion, and no lipid droplets were formed, and no apparent abnormalities were seen (Fig. 4A). In the HF group, lipid droplets of different sizes appeared, hepatocyte arrangement were disordered, and a few balloon-like changes were seen (Fig. 4B).

3.3. Ultrasonic image of ATT and UDFF

The unit of ATT value was dB/cm/MHz. The average ATT value of the NC group was 0.44 dB/cm/MHz at the beginning (week 0), and the average ATT value of the HF group was 0.42 dB/cm/MHz. At 32 weeks, the average ATT value in the NC group was 0.50 dB/cm/MHz, and the average ATT value in the HF group was 0.60 dB/cm/MHz. The UDFF value was expressed in %, with an initial (week 0) average UDFF value of 3.2% in the NC group and 2.8% in the HF group. At 32 weeks, the mean UDFF value in the NC group was 4.7%, and the mean UDFF value in the HF group was 12.1%. Representative ATT (Fig. 5A and B) and UDFF (Fig. 5C and D) measurement screens are shown in Fig. 5. In addition, pigs treated with high-fat diet showed significant ATT and UDFF observed values gain compared to control pigs (Fig. 6A and B).

3.4. Assessment diagnostic performance of ATT and UDFF

Spearman correlation analysis showed that ATT value was significantly correlated with NAS score ($r = 0.76$, $P < 0.001$). UDFF value was significantly correlated with the NAS score ($r = 0.80$, $P < 0.001$). Compared with the ultrasonic attenuation technique, the correlation coefficient between HRI and NAS score was slightly lower ($r = 0.62$, $P < 0.001$), but it was still statistically significant. In addition, ROC analysis showed that the AUC of ATT was 0.91 (95%CI, 0.84–0.99) ($P < 0.001$; Fig. 6C), the corresponding optimal diagnostic cut-off value was 0.59 dB/cm/MHz, the sensitivity was 88.5% and the specificity was 86.4%. The AUC of UDFF was 0.95 (95%CI, 0.90–1.00) ($P < 0.001$; Fig. 6D), the corresponding optimal diagnostic cut-off value was 5.5%, the sensitivity was 80.0%, and the specificity was 96.4%.

4. Discussion

In this study, we reported a novel NAFL model of Bama minipigs. The body weight and BMI of minipigs after high-fat feeding were significantly higher than that of minipigs fed an ordinary diet at the same period. The histological features of NAFL were characterized

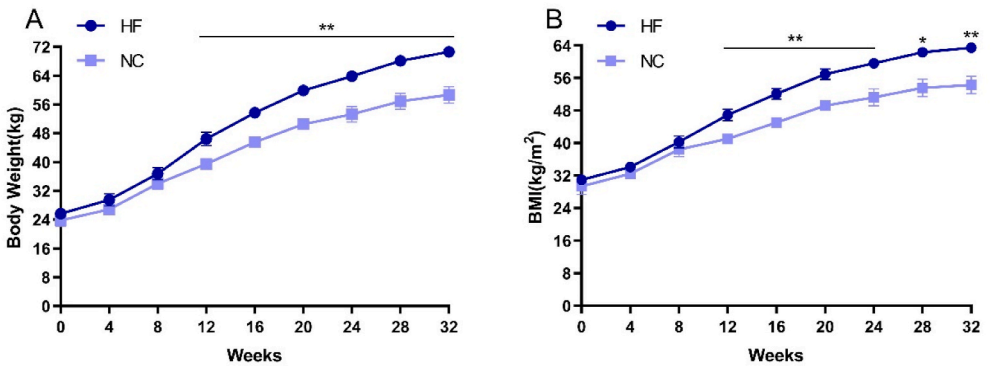

Fig. 2. Effects of high-fat diets on body weight and BMI. (A) The changes in body weight of the two groups of Bama minipigs. (B) The changes in BMI of the two groups of Bama minipigs. Note: Compared with the NC group, $^{*}P < 0.05$, $^{**}P < 0.01$.

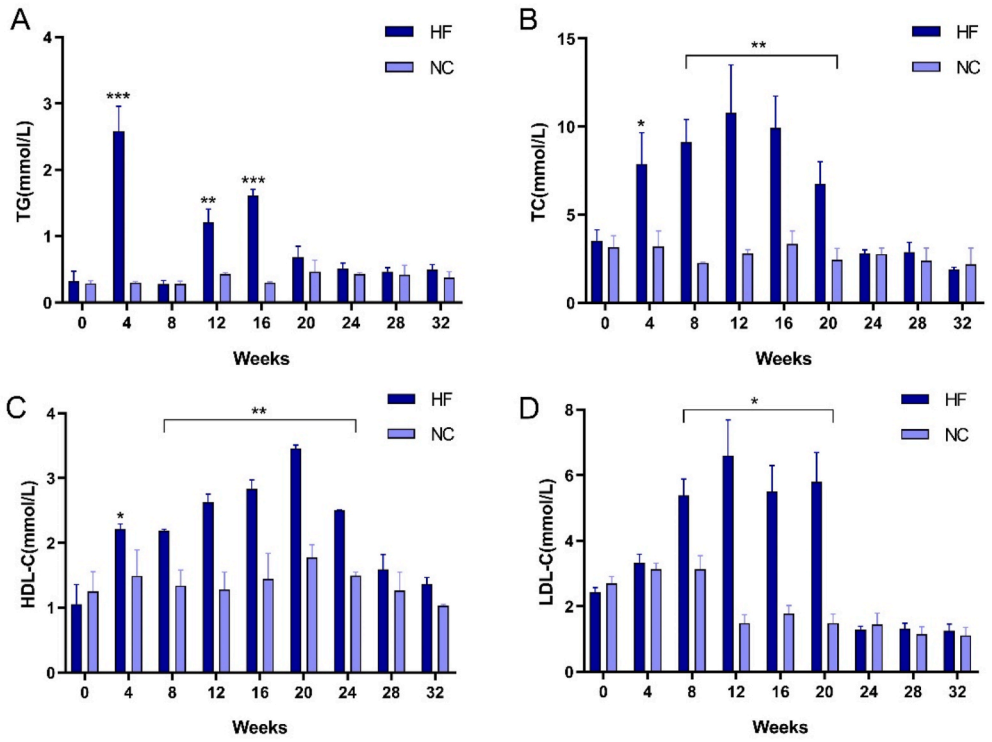

Fig. 3. Blood lipid levels in each group per week. (A to D) TG level (A), TC level (B), HDL-C level (C), and LDL-C level (D) in the two groups. Note: Compared with the NC group, $^{*}P < 0.05$, $^{**}P < 0.01$, $^{***}P < 0.001$.

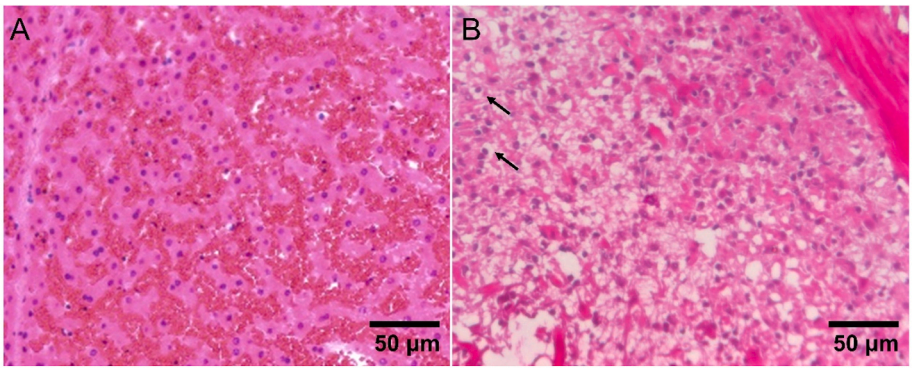

Fig. 4. Histopathological staining maps of the liver tissues of two groups at 32 weeks. (A) HE staining of the NC group. (B) HE staining of the HF group, balloon-like change was visible (arrow).

by a little balloon-like deformation of triglyceride lipid droplets and hepatocytes. Especially at 24 weeks after the start of high-fat feeding, the minipigs developed and shown typical triglyceride lipid droplets and balloon-like changes. Despite there being no significant difference in serum ALT, AST, GGT, ALB, and GLB between the HF group and the NC group during the experiment, TG, TC, and HDL-C showed significant differences after four weeks of high-fat induction. In addition, the ultrasonic attenuation parameters ATT and UDFF measured were highly correlated with pathological results. These features make this model attractive and reliable for further research on NAFL.

Advantages of the mouse models include a relatively short study time and low cost, compared to large animal models. Therefore, most previous experiments used mice as research objects in animal model studies. A review in 2019 systematically outlined a NAFLD/NASH model in mice [11]. They suggested that mouse models of NASH should exhibit weight gain, abnormal lipid distribution, and hyperinsulinemia due to insulin resistance. In a large animal model study of steatohepatitis caused by dietary control, which quite closely summarizes NAFLD in humans [21], in their experiment, compared with the control group, there was a specific statistical difference in blood lipid levels between the high-fructose group and the high-fat group. In the high-fructose group, TC increased, but LDL-C decreased, while in the high-fat group, TC, TG, HDL-C, and LDL-C levels all increased, similar to our experimental results. In

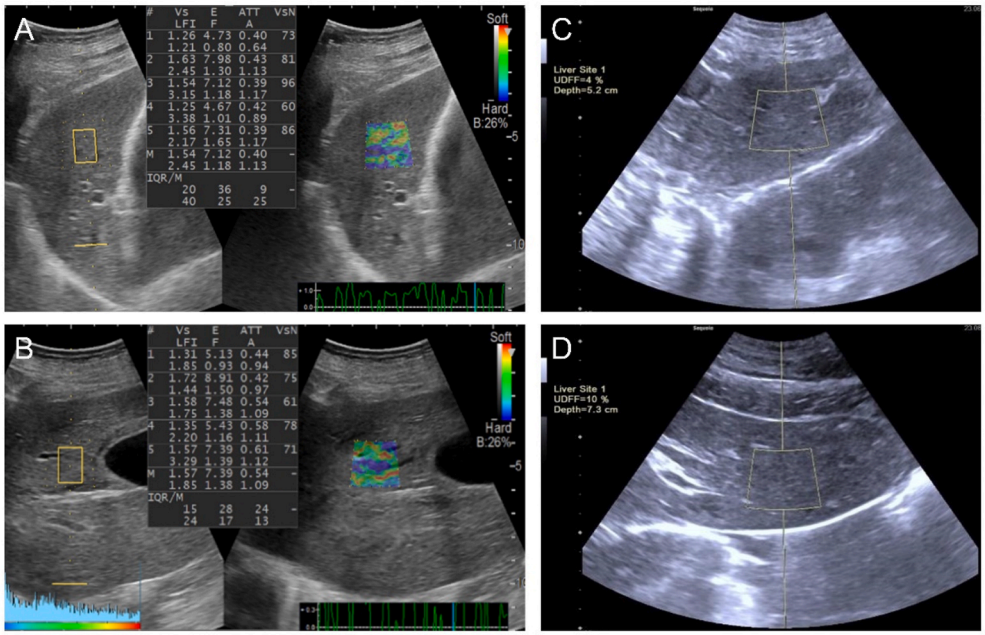

Fig. 5. Representative ATT and UDFF measurement screens (A–D). (A) The ATT measurement in the NC group at week 16 was 0.45 dB/cm/MHz. (B) The ATT measurement in the HF group at week 16 was 0.54 dB/cm/MHz. (C) In the NC group at 32 weeks, the UDFF value of a successful measurement is 4% (a case). (D) In the HF group at 32 weeks, the UDFF value of a successful measurement is 10% (a case).

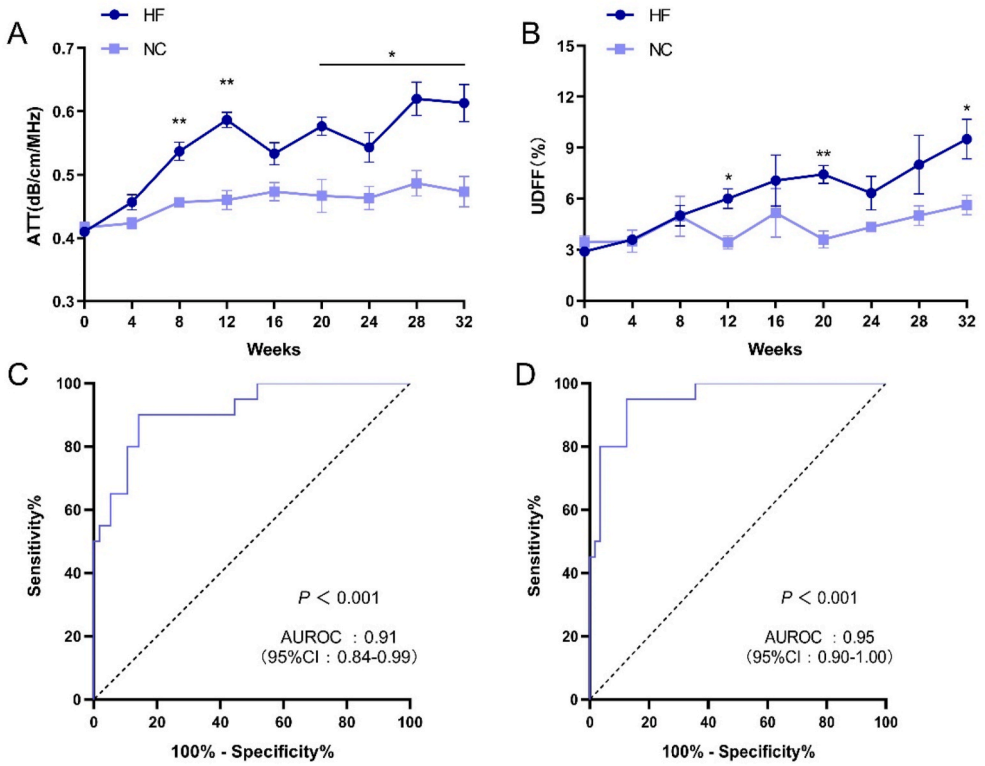

Fig. 6. Trends of ATT and UDFF during the experiment and ROC curves. (A) Trends in ATT measurements over time in the two groups. (B) Trends in UDFF measurements over time in the two groups. (C) ROC curve of ATT. (D) ROC curve of UDFF.

another study on guinea pigs [22], dietary induction of dyslipidemia leads to NAFLD in guinea pigs, TC in both the high-fat group and high-fat and high-sugar group peaked at 22 weeks and then declined. TC in the HF group in our study began to decline after reaching a peak at 12 weeks, but the statistical difference from the NC group persisted up to 20 weeks. These confirmed the effects of diet and time on TC plasma levels. In addition, differences in lipid levels were not essentially statistically significant between 24 and 32 weeks. This finding was similar to the previous study in pig model [23], in which there was no consecutive statistical difference in TG, LDL between the high-fat diet group and the control group. Moreover, an interesting finding in our study was that the Bama minipigs in the HF group showed liver steatosis without significant changes in liver transferase. This result indicated that elevated liver transferase may not be a prerequisite for hepatic steatosis.

Although there are insurmountable differences between non-human species and humans, animal models should mimic the development of human diseases. Diet-induced obesity is one of the disease risk factors for human NAFLD [24]. Thus, dietary compositions should be broadly similar to the human diet in terms of macronutrient composition and should not contain unnatural toxins, such as the use of high levels of cholesterol or fat. Therefore, the whole experiment was performed under the guide of feeding induction without using carbon tetrachloride, which can cause steatosis. In addition, the model should develop a liver phenotype similar to human disease.

Accurate assessment of steatosis is essential for the management of patients with chronic liver disease in clinical practice, as well as for epidemiological and therapeutic studies in clinical studies. Although the magnetic resonance proton fat density fraction (MRI-PDFF) has high accuracy [25,26], screening large numbers of patients is challenging. Consequently, alternative methods are needed for the initial diagnosis of steatosis. The ideal method for assessing steatosis should be widely available, non-invasive, safe, sensitive, accurately quantifiable, repeatable, and affordable [27]. A Japanese study [28] included 351 patients with pathologically confirmed steatosis, it was concluded that the median ATT value of mild hepatic steatosis was 0.63 dB/cm/MHz, and the ATT value increased with the increase of fat content. A recent study was conducted in the United States to evaluate the quantitative effectiveness of UDFF in detecting hepatic steatosis and liver fat content [29], using MRI-PDFF as reference standard, it is found that UDFF and MRI-PDFF had high consistency, and the correlation coefficient was as high as 0.81. Noninvasive ultrasonography is the preferred method to evaluate the grading of fatty liver. However, mice livers are so small that even if pathological changes occur, they are difficult to detect on imaging. Therefore, this study selected pigs as the carrier of the animal model of fatty liver. On the one hand, the size of pig liver is larger and closer to that of human liver, on the other hand, pig liver segmentation is similar to human liver segmentation. Importantly, unlike human phenotypic studies, where sampling is usually limited to a single point in time, animal models allow for the collection of sufficient tissue to reduce sampling errors and track physiological and imaging changes during disease progression or reversal. Indeed, large animal models are expensive and can only be developed and used by centers with special resources and expertise. Still, large animal models provide the opportunity for a series of examinations of the same group of animals, and physiological characteristics, such as heart anatomy, body size, propensity for sedentary behavior, and dietary carbohydrate and lipid metabolism, are more similar to humans in pigs than in rodents. Compared with domestic pigs, miniature pigs have advantages in size, feeding cost, and space requirements [30]. In addition, our study design still has some limitations. First, due to practical problems, experimental funding, and limited lab space to house large numbers of pigs at once, our groups were not matched in terms of numbers or gender. Secondly, we acknowledge that there were some differences between our high-fat diet and the high-fat diet in the previous literature, which cannot be uniform and was not ideal from a methodological point of view. However, it did not affect our goal of inducing the NAFL phenotype in animals. Finally, for the QUS measurement, we only divided the truncation value of mild fatty liver because moderate to severe steatosis rarely appeared in pathological findings.

In summary, we established an animal model of hepatic steatosis highly similar to human NAFL from a histological, imaging, and metabolic perspective. This model will offer an exceptional opportunity to evaluate the effectiveness of innovative therapeutic agents. Furthermore, we evaluated the diagnostic efficacy of emerging QUS, both ATT and UDFF had excellent ability to distinguish hepatic steatosis. We discovered that ATT had higher sensitivity while UDFF had higher specificity. The two methods can reliably quantify the liver fat content and improve the diagnostic value of ultrasonic detection of hepatic steatosis.

Financial support

Supported by Nanjing Health Commission, China (project number: YKK21275).

Data availability statement

The data that support the findings of this study are available from the corresponding author, upon request.

CRediT authorship contribution statement

Huihui Chen: Writing – original draft, Visualization, Validation, Investigation. **Huiming Shen:** Resources, Methodology, Conceptualization. **Jiahao Han:** Methodology, Investigation. **Pingping Wang:** Methodology. **Danlei Song:** Methodology. **Hongyuan Shen:** Methodology. **Xiaoying Wei:** Methodology. **Bingjie Yang:** Writing – review & editing, Supervision. **Jia Li:** Writing – review & editing, Supervision, Conceptualization.

Declaration of competing interest

The authors declare that they have no known competing financial interests or personal relationships that could have appeared to influence the work reported in this paper.

References

[1] S.K. Sarin, M. Kumar, M. Eslam, J. George, M. Al Mahtab, S.M.F. Akbar, et al., Liver diseases in the Asia-Pacific region: a Lancet Gastroenterology & Hepatology commission, Lancet Gastroenterol. Hepatol. 5 (2020) 167–228.

[2] S. Singh, A.M. Allen, Z. Wang, L.J. Prokop, M.H. Murad, R. Loomba, Fibrosis progression in nonalcoholic fatty liver vs nonalcoholic steatohepatitis: a systematic review and meta-analysis of paired-biopsy studies, Clin. Gastroenterol. Hepatol. 13 (2015) 643–654.

[3] R. Bharath, P. Rajalakshmi, M.A. Mateen, Multi-modal framework for automatic detection of diagnostically important regions in nonalcoholic fatty liver ultrasonic images, Biocybern. Biomed. Eng. 38 (2018) 586–601.

[4] S.K. Kamarajah, W.K. Chan, N.R.N. Mustapha, S. Mahadeva, Repeated liver stiffness measurement compared with paired liver biopsy in patients with non-alcoholic fatty liver disease, Hepatol. Int. 12 (2018) 44–55.

[5] R. Pais, F. Charlotte, L. Fedchuk, P. Bedossa, P. Lebray, T. Poynard, et al., A systematic review of follow-up biopsies reveals disease progression in patients with non-alcoholic fatty liver, J. Hepatol. 59 (2013) 550–556.

[6] E.M. Brunt, A.D. Clouston, Z. Goodman, C. Guy, D.E. Kleiner, C. Lackner, et al., Complexity of ballooned hepatocyte feature recognition: defining a training atlas for artificial intelligence-based imaging in NAFLD, J. Hepatol. 76 (2022) 1030–1041.

[7] N.S. Samji, R. Verma, S.K. Satapathy, Magnitude of nonalcoholic fatty liver disease: western perspective, J Clin Exp Hepatol 9 (2019) 497–505.

[8] P.K. Santhekadur, D.P. Kumar, A.J. Sanyal, Preclinical models of non-alcoholic fatty liver disease, J. Hepatol. 68 (2018) 230–237.

[9] C.R. Muller, A.T. Williams, A.M. Eaker, F. Dos Santos, A.F. Palmer, P. Cabrales, High fat high sucrose diet-induced dyslipidemia in Guinea pigs, J. Appl. Physiol. 130 (2021) 1226–1234.

[10] T. Yamada, Y. Kashiwagi, T. Rokugawa, H. Kato, H. Konishi, T. Hamada, et al., Evaluation of hepatic function using dynamic contrast-enhanced magnetic resonance imaging in melanocortin 4 receptor-deficient mice as a model of nonalcoholic steatohepatitis, Magn. Reson. Imaging 57 (2019) 210–217.

[11] G. Farrell, J.M. Schattenberg, I. Leclercq, M.M. Yeh, R. Goldin, N. Teoh, et al., Mouse models of nonalcoholic steatohepatitis: toward optimization of their relevance to human nonalcoholic steatohepatitis, Hepatology 69 (2019) 2241–2257.

[12] S.N. Heinritz, R. Mosenthin, E. Weiss, Use of pigs as a potential model for research into dietary modulation of the human gut microbiota, Nutr. Res. Rev. 26 (2013) 191–209.

[13] R. Manjarín, K. Dillard, M. Coffin, G.V. Hernandez, V.A. Smith, T. Noland-Lidell, et al., Dietary fat composition shapes bile acid metabolism and severity of liver injury in a pig model of pediatric NAFLD, Am. J. Physiol. Endocrinol. Metab. 323 (2022) E187–E206.

[14] P.K. Hsu, L.S. Wu, H.H. Yen, H.P. Huang, Y.Y. Chen, P.Y. Su, et al., Attenuation imaging with ultrasound as a novel evaluation method for liver steatosis, J. Clin. Med. 10 (2021) 9.

[15] R.G. Barr, S.R. Wilson, D. Rubens, G. Garcia-Tsao, G. Ferraioli, Update to the society of radiologists in ultrasound liver elastography consensus statement, Radiology 296 (2020) 263–274.

[16] R.H. Marshall, M. Eissa, E.I. Bluth, P.M. Gulotta, N.K. Davis, Hepatorenal index as an accurate, simple, and effective tool in screening for steatosis, Am. J. Roentgenol. 199 (2012) 997–1002.

[17] M.P. Frankland, J.R. Dillman, C.G. Anton, B.D. Coley, M.P. Nasser, S.M. O'Hara, et al., Diagnostic performance of ultrasound hepatorenal index for the diagnosis of hepatic steatosis in children, Pediatr. Radiol. 52 (2022) 1306–1313.

[18] J.K.C. Lau, X. Zhang, J. Yu, Animal models of non-alcoholic fatty liver disease: current perspectives and recent advances, J. Pathol. 241 (2017) 36–44.

[19] D.E. Kleiner, E.M. Brunt, M. Van Natta, C. Behling, M.J. Contos, O.W. Cummings, et al., Design and validation of a histological scoring system for nonalcoholic fatty liver disease, Hepatology 41 (2005) 1313–1321.

[20] A.J. Sanyal, E.M. Brunt, D.E. Kleiner, K.V. Kowdley, N. Chalasani, J.E. Lavine, et al., Endpoints and clinical trial design for nonalcoholic steatohepatitis, Hepatology 54 (2011) 344–353.

[21] L. Lee, M. Alloosh, R. Saxena, W. Van Alstine, B.A. Watkins, J.E. Klaunig, et al., Nutritional model of steatohepatitis and metabolic syndrome in the ossabaw miniature swine, Hepatology 50 (2009) 56–67.

[22] P. Tveden-Nyborg, M.M. Birck, D.H. Ipsen, T. Thiessen, L.D. Feldmann, M.M. Lindblad, et al., Diet-induced dyslipidemia leads to nonalcoholic fatty liver disease and oxidative stress in Guinea pigs, Transl. Res. 168 (2016) 146–160.

[23] Y.Q. Zhao, M.M. Niu, Y.X. Jia, J.F. Yuan, L. Xiang, X. Dai, et al., Establishment of type 2 diabetes mellitus models using streptozotocin after 3 months high-fat diet in Bama minipigs, Anim. Biotechnol. 34 (2023) 2295–2312.

[24] H.M. Al-Dayyat, Y.M. Rayyan, R.F. Tayyem, Non-alcoholic fatty liver disease and associated dietary and lifestyle risk factors, Diabetes Metab. Syndrome-Clin. Res. Rev. 12 (2018) 569–575.

[25] C.C. Park, P. Nguyen, C. Hernandez, R. Bettencourt, K. Ramirez, L. Fortney, et al., Magnetic resonance elastography vs transient elastography in detection of fibrosis and noninvasive measurement of steatosis in patients with biopsy-proven nonalcoholic fatty liver disease, Gastroenterology 152 (2017) 598–607.

[26] P. Bannas, H. Kramer, D. Hernando, R. Agni, A.M. Cunningham, R. Mandal, et al., Quantitative magnetic resonance imaging of hepatic steatosis: validation in *ex vivo* human livers, Hepatology 62 (2015) 1444–1455.

[27] K. Imajo, H. Toyoda, S. Yasuda, Y. Suzuki, K. Sugimoto, H. Kuroda, et al., Utility of ultrasound-guided attenuation parameter for grading steatosis with reference to MRI-PDFF in a large cohort, Clin. Gastroenterol. Hepatol. 20 (2022) 2533–2541.e2537.

[28] N. Tamaki, Y. Koizumi, M. Hirooka, N. Yada, H. Takada, O. Nakashima, et al., Novel quantitative assessment system of liver steatosis using a newly developed attenuation measurement method, Hepatol. Res. 48 (2018) 821–828.

[29] R. De Robertis, F. Spoto, D. Autelitano, D. Guagenti, A. Olivieri, P. Zanutto, et al., Ultrasound-derived fat fraction for detection of hepatic steatosis and quantification of liver fat content, Radiol. Med. 128 (2023) 1174–1180.

[30] S.J. Li, S.T. Ding, H.J. Mersmann, C.H. Chu, C.D. Hsu, C.Y. Chen, A nutritional nonalcoholic steatohepatitis minipig model, JNB (J. Nutr. Biochem.) 28 (2016) 51–60.